Hindawi Publishing Corporation
Indian Journal of Materials Science
Volume 2014, Article ID 396147, 7 pages
http://dx.doi.org/10.1155/2014/396147

Research Article

Ytterbium Doped Gadolinium Oxide (Gd_2O_3:Yb^{3+}) Phosphor: Topology, Morphology, and Luminescence Behaviour

Raunak Kumar Tamrakar,[1] Durga Prasad Bisen,[2] Chandra Shekher Robinson,[1] Ishwar Prasad Sahu,[2] and Nameeta Brahme[2]

[1] *Department of Applied Physics, Bhilai Institute of Technology (Seth Balkrishan Memorial), Near Bhilai House, Durg 491001, India*
[2] *School of Studies in Physics and Astrophysics, Pt. Ravishankar Shukla University, Raipur 492010, India*

Correspondence should be addressed to Raunak Kumar Tamrakar; raunak.ruby@gmail.com

Received 12 December 2013; Accepted 4 February 2014; Published 3 April 2014

Academic Editors: Y. Huttel and A. Kajbafvala

Gd_2O_3:Yb^{3+} phosphor has been synthesized by the solid state reaction method with boric acid used as a flux. The resulting Gd_2O_3:Yb^{3+} phosphor was characterized by X-ray diffraction (XRD) technique, Fourier transmission infrared spectroscopy (FTIR), scanning electron microscope (SEM) and transmission electron microscope (TEM), and photoluminescence and thermoluminescence. The results of the XRD show that obtained Gd_2O_3:Yb^{3+} phosphor has a cubic structure. The average crystallite sizes could be calculated as 42.9 nm, confirmed by the TEM results. The study suggested that Yb^{3+} doped phosphors are potential luminescence material for IR laser diode pumping.

1. Introduction

Luminescent materials in various forms such as colloidal, bulk, nano, crystals, and nanocrystals are of interest not only for basic research, but also for interesting application [1–3]. Rare earth activated phosphors have attracted great interest because of their marked improvements in lumen output, color rendering index, and energy efficiency, and greater radiation stability Lanthanum oxide (La_2O_3) is recognized as an excellent host material for rare earth (RE) with luminescence applications with a relatively low cost. These phosphors have been recognized to hold tremendous potential in the field of photonic applications. The doping concentration is controlled over a broad range without the host structure influence. The luminescent properties of RE in La_2O_3 nanocrystalline powders using different synthesis methods have been recently reported [4, 5]. Gd_2O_3 is an Ln_2O_3-type oxide. The Ln_2O_3 (Ln = Gd, Y, Sc, Lu, Dy, etc.) oxides have been extensively studied because of their optoelectronic and display applications. Gadolinium oxide (Gd_2O_3) has been studied widely as the host matrix for downconversion [6–8] processes because of its interesting physical properties, such as high melting point (2320°C), chemical durability, thermal stability, and low phonon energy (~600 cm^{-1}). Gd_2O_3 hosts have smaller phonon energies compared to hosts such as YAG or YAP; smaller phonon energies lead to a reduction in nonradiative losses and hence lead to increases in the luminescence efficiency [9, 10].

The Yb^{3+} ion has several advantages compared with other rare earth ions due to its very simple energy level scheme, constituting of only two $^2F_{5/2}$ and $^2F_{7/2}$ levels. There is no excited state absorption, no cross-relaxation process, and no more upconversion internal mechanism able to reduce the effective laser cross section and, in addition, the intense and broad Yb^{3+} absorption lines are well suited for IR laser diode pumping. The luminescence emission of RE ions is the result of unique electronic transitions, and different emission colors can be achieved by the controlled doping of specific lanthanide ions into the Gd_2O_3 host matrix. Yb^{3+} ions attracted us because of their simple energy level diagram, having two states $^2F_{5/2}$ and $^2F_{7/2}$ with an energy difference of 10,000 cm^{-1}. Yb^{3+} ions are commonly used to activate materials and serve as a useful probe of host characteristics

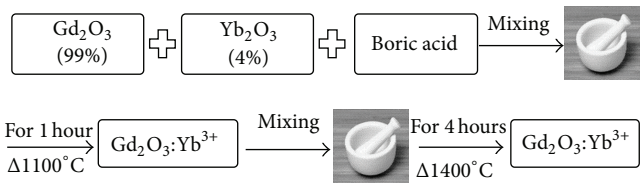

Scheme 1: Synthesis of Gd_2O_3:Yb^{3+} phosphor.

as their luminescence is known to be highly sensitive to the coordination of the activator site because Yb^{3+} ions have a large absorption cross section [11]. In the present study, we were focused on synthesis of Gd_2O_3:Yb^{3+} phosphors by solid state reaction method and on investigating the luminescence behaviour of the prepared phosphor.

In this work, we report the solid state synthesis of ytterbium doped Gd_2O_3 phosphor. Gd_2O_3:Yb^{3+} phosphor was investigated by X-ray diffraction (XRD), field emission scanning electron microscopy (FESEM), Fourier transform infrared spectroscopy (FTIR), and thermoluminescence (TL) and photoluminescence (PL) measurements.

1.1. Solid State Synthesis of Gd_2O_3:Yb^{3+} Phosphor. Gd_2O_3:Yb^{3+} phosphor was synthesized by conventional solid state method. Oxide of rare earth materials such as gadolinium oxide (Gd_2O_3), ytterbium oxide (Yb_2O_3), and boric acid as a flux with high purity (99.99%) were used as precursor materials to prepare Yb^{3+} doped Gd_2O_3 phosphor. In stoichiometric ratios of rare earth ions Yb^{3+} (4 mole%) and Gd_2O_3 were used to synthesize Gd_2O_3:Yb^{3+} phosphor. These chemicals were weighed and ground into a fine powder by using agate mortar and pestle. The ground sample was placed in an alumina crucible and heated at 1100°C for 1 hour followed by dry grinding and further heated at 1400°C for 4 hours in a muffle furnace. The sample is allowed to cool at room temperature in the same furnace for about 15 h [12–14] (see Scheme 1).

1.2. Characterization of Prepared Phosphor. Crystalline phases and sizes of as-prepared phosphors were characterized by powder X-ray diffraction (XRD; Bruker D8 Advance). The morphology and particle sizes of Gd_2O_3:Yb^{3+} phosphor were observed by transmission electron microscopy (Philips CM-200) and FE-SEM (JSM-7600F). Photoluminescence measurements were performed using a Spectrofluorophotometer. TL glow curve was recorded at room temperature by using TLD reader I1009 (Nucleonix Sys. Pvt. Ltd. Hyderabad). All of the measurements were performed at room temperature.

2. Results and Discussion

2.1. XRD Analysis Results. Figure 1 shows the XRD pattern of Yb^{3+} doped Gd_2O_3 phosphor. The average particles size was calculated by Debye-Scherrer formula [15]:

$$D = \frac{k\lambda}{\beta \operatorname{Cos} \theta}, \quad (1)$$

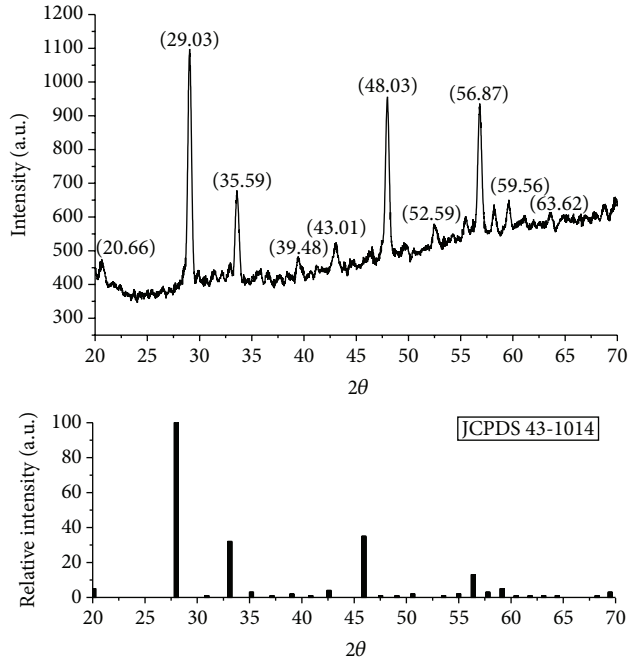

Figure 1: XRD result of Gd_2O_3:Yb^{3+} and JCPDS card 43-1014 for cubic Gd_2O_3.

Table 1: (h, k, l) and d spacing (Å) of Gd_2O_3:Yb^{3+}.

Serial number	2θ	(h, k, l)	d spacing (Å)
1	20.66	(2, 1, 1)	4.315
2	29.03	(2, 2, 2)	3.071
3	35.59	(4, 1, 1)	2.666
4	39.48	(3, 3, 2)	2.284
5	43.01	(1, 3, 4)	2.096
6	48.03	(4, 4, 0)	1.894
7	52.59	(6, 1, 1)	1.743
8	56.87	(6, 2, 2)	1.617
9	59.56	(4, 4, 4)	1.55
10	63.62	(6, 3, 3)	1.461

where k is a dimensionless constant, λ is the wavelength of X-ray used, β is the full width at half maxima (FWHM) of the diffraction peak, and θ is the diffraction angle (Bragg's angle) for the (h, k, l) plane. The observed values are in good agreement with the standard values given for the cubic structure. X-ray diffraction pattern of Yb^{3+} doped Gd_2O_3 confirms proper phase formation and nanocrystalline nature of the sample. All the diffraction peaks are in agreement with those of the JCPDS card number 43-1014 for Yb^{3+} doped and confirm that the sample has a cubic structure [16]. Particle size of the prepared sample is found to be 41 nm. The values of interplanar spacing d for cubic phase structure are calculated by reported formulas [17]:

$$d = \frac{a}{\sqrt{h^2 + k^2 + l^2}}, \quad (2)$$

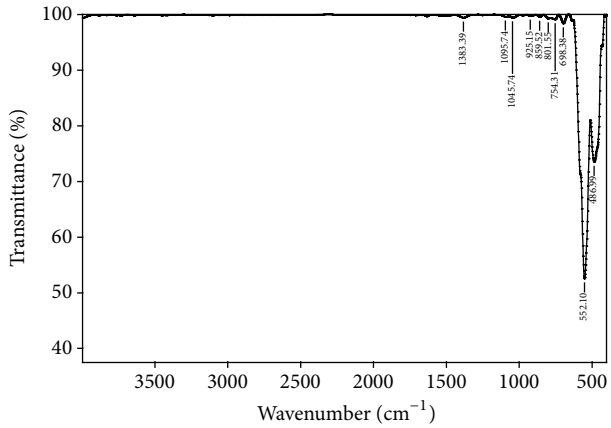

FIGURE 2: Fourier transform infrared (FTIR) spectra of Gd_2O_3:Yb^{3+}.

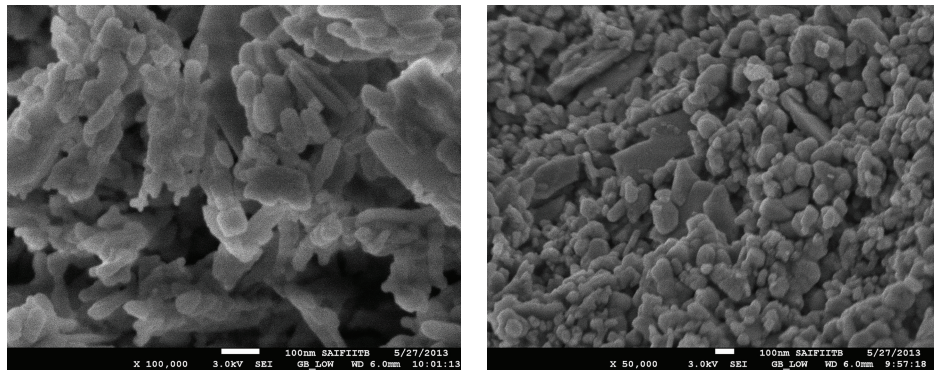

(a) (b)

FIGURE 3: FEG-SEM images of Gd_2O_3:Yb^{3+}.

where d is the interplanar spacing. d spacing and (h, k, l) value for different theta were also calculated (Table 1).

2.1.1. Fourier Transform Infrared (FTIR) Spectroscopy Analysis. The Fourier transform infrared (FTIR) spectra of ytterbium doped Gd_2O_3 phosphor were recorded in order to investigate different molecular species present in the phosphor and are shown in Figure 2. Here Fourier transform infrared (FTIR) spectra were measured via the potassium bromide (KBr) pallet formation by pellet technique. The bands around 440 and 542 cm^{-1} are assigned to the Gd–O vibration of cubic Gd_2O_3 [18]. All the observed peaks confirm the formation of Yb^{3+} doped Gd_2O_3 phosphor.

2.1.2. Field Emission Gun Scanning Electron Microscope (FEG-SEM) Results. The FEG-SEM images of the product obtained are shown in Figures 3(a) and 3(b). The as-prepared Gd_2O_3:Yb^{3+} phosphor has a dumble-like morphology with an average diameter of 40–50 nm. It can be found that the product is composed of many sphere shaped particles and some of them are agglomerated together. The average particle size was calculated by collecting 100 clearly identifiable particles estimated to be 42.9 nm (Figure 4).

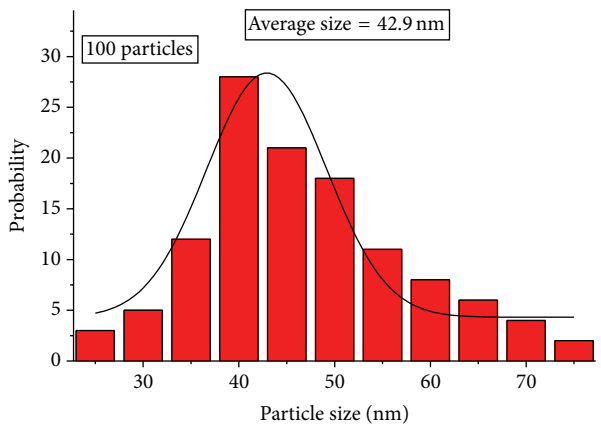

FIGURE 4: Histogram of particle size distribution for the studied Gd_2O_3:Yb^{3+} phosphors.

The statistic histogram is shown in Figure 4 where the Gaussian fitting was also carried out. The difference between the average size confirmed from FEG-SEM and the crystallographic size derived from XRD is probably due to the reasons that, on one hand, the crystallographic size calculation based

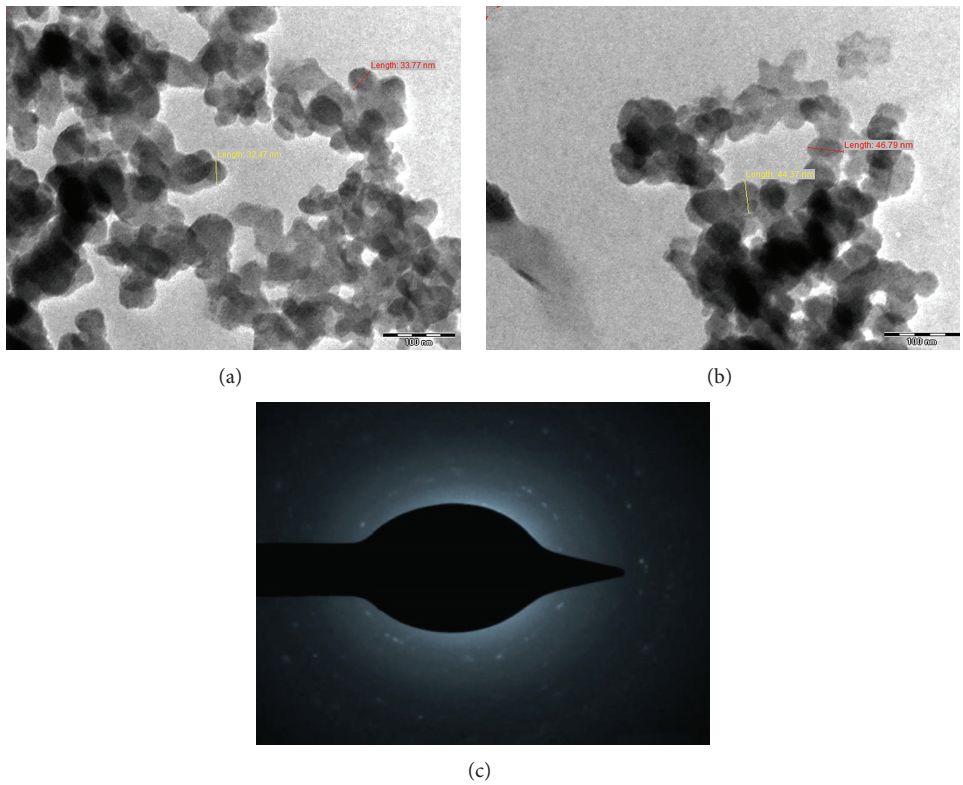

(a) (b)

(c)

FIGURE 5: Transmission electron micrographs of Gd_2O_3:Yb^{3+} (a and b) along with the SAED (c) pattern.

on the Debye-Scherrer equation in the case of larger size particles may introduce larger error and that, on the other hand, the crystallographic size reflects the size of well-crystallized part of the particles, but the average size observed from FEG-SEM presents the apparent size of the particles; thus, they may be different.

2.2. Transmission Electron Microscope (TEM) Result. Figure 5 shows the TEM micrographs of the Gd_2O_3:Yb^{3+} phosphor along with the selected area electron diffraction SAED pattern. The TEM measurements were carried out at different points of the grid and almost similar results were obtained each time. The TEM image shows the presence of spherical nanoparticles with an average diameter lying in between 32 and 44 nm. The crystalline nature of the material is clear from the SAED pattern. A variation of the average diameter of nanoparticles in between such a small range can be considered roughly as the nearly uniform distribution. From the TEM image, it can also be clearly observed that crystals present in the phosphor material are highly agglomerated. The selected area electron diffraction pattern (SAED) (inset c) shows the bright spots, which indicates the high crystalline nature of the phosphor material. Indexing of the SAED pattern also confirms the presence of the cubic Gd_2O_3 phase.

2.2.1. Thermoluminescence Glow Curve of Gd_2O_3:Yb^{3+} Phosphor. Thermoluminescence (TL) is a convenient technique of studying optically active centers in solids. Energy absorbed by the solid is emitted as light is measured in the heating process and in turn the light is measured in the form of glow curve. From the shape position and intensity of the glow curve, various defect characteristics, in particular trap depth, are calculated by different methods. TL is a phenomenon which is caused by the thermally assisted release of the irradiation induced electrons from the traps of the material. In the structure of the most insulating solids, there exist point defects, naturally occurring or artificially created, which induce electronic states in the forbidden band. These defects have great importance in understanding the thermoluminescence (TL) phenomenon. Several models exist, which explain the basic principles of the TL process using charge carrier traps induced by impurities called dopants. Thermoluminescence (TL) is a superbly sensitive technique to record radiation history in insulators and it is consequently widely used in radiation dosimetry and archeological dating, as well as for studies of crystalline defects. These models provide diagnostic tools that can be employed to evaluate the TL kinetic parameters using processes based on electronic transitions of the charge carriers. Crystalline TL materials exhibit a glow curve with one or more peaks when the charge carriers are released. This glow curve is a graphical representation of the luminescence intensity as a function of time or temperature, providing information about parameters corresponding to each peak, such as activation energy, frequency factor, and the order of the kinetics [19, 20]. The TL curve can provide valuable information on the intrinsic defect of materials and the energetic ray to which the material was subjected. TL glow curve for Gd_2O_3:Yb^{3+} phosphor was recorded with a UV

Table 2: Kinetic parameters of Gd_2O_3:Yb^{3+} TL glow curve.

UV exposure time	T_1	T_m	T_2	τ	δ	ω	$\mu = \delta/\omega$	Activation energy E in eV	Frequency factor S in s^{-1}
5	101.9	132.4	170.1	30.67	37.77	68.44	0.552	0.704	7.9×10^9

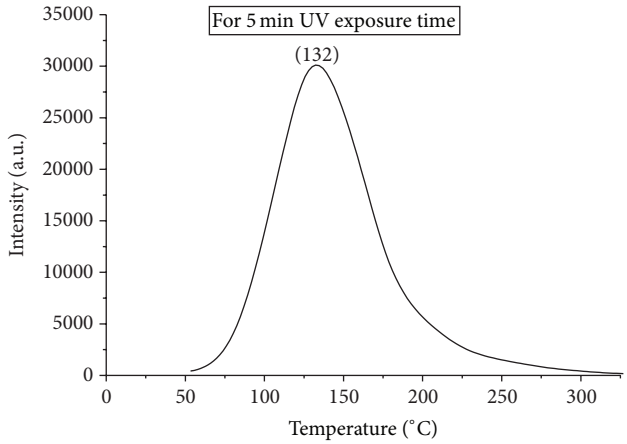

Figure 6: TL glow curved result of Gd_2O_3:Yb^{3+}.

exposure of 5 min at a heating rate 6.7°C s^{-1}. The order of kinetics and the activation energy with frequency factor are calculated using Chen's empirical formula [21–23]. Figure 6 shows the TL glow curve of Gd_2O_3:Yb^{3+} for 5 Min UV exposure time. In the glow curve, only a single peak was observed, at around 132.37°C.

The kinetic parameters of Gd_2O_3:Yb^{3+} phosphor are listed in Table 2. In this TL glow curve shape factor $\mu \sim 0.52$ or greater than second-order kinetics, which may be caused by the presence of two or more traps with similar trap energies. Here the value of μ is 0.552 for 5 minutes, which shows the second-order kinetics. The value of activation energy belongs to 0.704 eV and frequency factor 7.9×10^9 s^{-1}.

2.3. Photoluminescence Studies. The absorption and emission spectra of Gd_2O_3:Yb^{3+} phosphor were recorded at room temperature (Figures 7(a) and 7(b)). There is a large overlap observed between absorption and emission spectra. Several lines can be seen in both absorption and emission due to the different transitions between the two $^2F_{7/2}$ and $^2F_{5/2}$ multiplets. The energy level scheme of Yb^{3+} is very simple and contains two multiplets, the ground $^2F_{7/2}$ state and the excited $^2F_{5/2}$ state. The strong interaction of Yb^{3+} ions with the lattice vibration gives rise to strong vibronic sidebands or even to supplementary Stark levels and phonon which can easily be taken for the assignment of electronic transitions.

There are seven Stark levels distributed in the two manifolds and labeled from 1 to 4 in ground state and from 5 to 7 in excited state from the lowest to highest energy. The strong electron-phonon coupling of Yb^{3+} ion is responsible for the additional peaks which appear in emission spectra. The resonant transition appears at 981 nm corresponding to the zero phonon line transition between Stark level 1 → 5

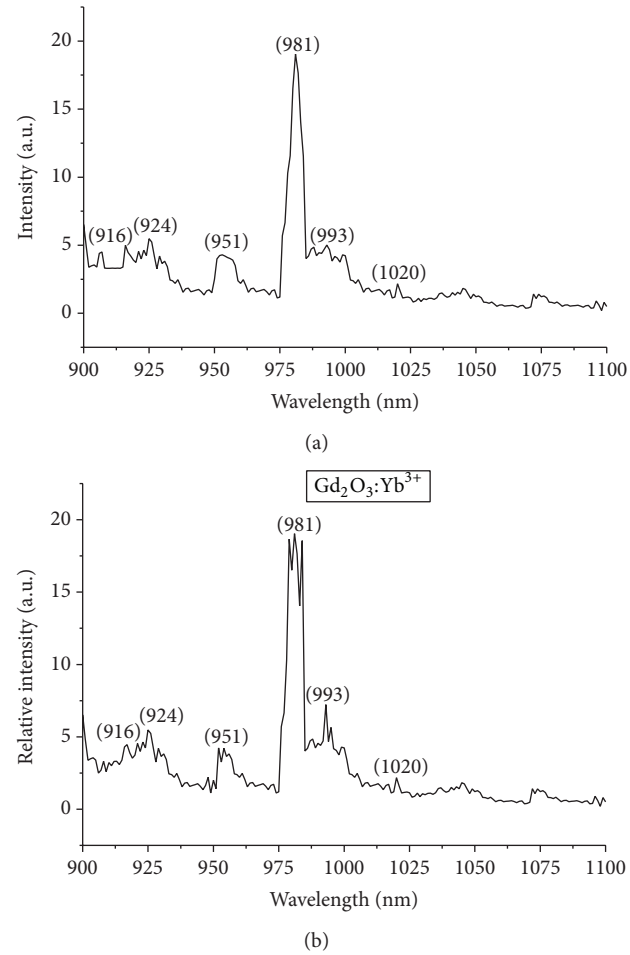

Figure 7: (a) Absorption PL spectra of Gd_2O_3:Yb^{3+} (4 mol%). (b) Emission PL spectra of Gd_2O_3:Yb^{3+} (4 mol%).

and at 1020 nm is due to 5 → 3 emission transition. At first attempt, the 1–7 and 1–6 lines are located at 924 nm and 916 nm, respectively [24–26]. In absorption spectra at room temperature, the transitions from the $^2F_{7/2}$ ground state thermally populated Stark levels are clearly seen and fit well with the corresponding emission transitions. The observed peaks are the result of absorption from mainly 1, 2, and 3 populated stark levels. The energy level scheme of Yb^{3+} helps to explain the above-mentioned transitions between Stark levels (Figure 8).

3. Conclusion

The cubic face Yb^{3+} doped Gd_2O_3 phosphor was successfully synthesized by the solid state reaction method, which is confirmed by the XRD result well matched with JCPDS card.

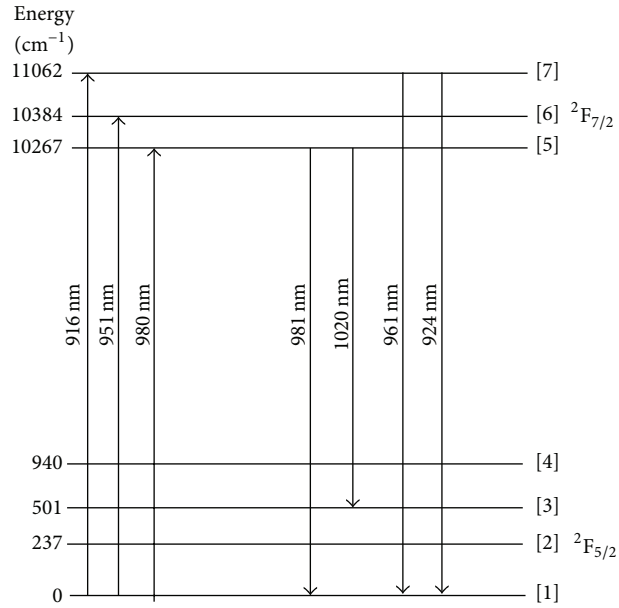

FIGURE 8: Crystal field energy level scheme for Gd_2O_3:Yb^{3+}.

The SEM and TEM results agree with the XRD result. The PL emission spectra show that the peak at 981 nm corresponds to the transition from one the stark level of $^2F_{7/2}$ to the lowest level of multiplet $^2F_{5/2}$. In TL glow curve, only a single peak was observed, at around 132°C. The value of activation energy belongs to 0.704 eV and frequency factor 7.9×10^9 s^{-1}.

Conflict of Interests

The authors declare that there is no conflict of interests regarding the publication of this paper.

Acknowledgments

The authors are very grateful to IUC Indore for XRD characterization and also thankful to Dr. Mukul Gupta for his cooperation. The authors are very thankful to SAIF, IIT, Bombay, for other characterizations such as SEM, TEM, and FTIR.

References

[1] C. Feldmann, T. Jüstel, C. R. Ronda, and P. J. Schmidt, "Inorganic luminescent materials: 100 Years of research and application," *Advanced Functional Materials*, vol. 13, no. 7, pp. 511–516, 2003.

[2] M. K. Devaraju, S. Yin, and T. Sato, "A rapid hydrothermal synthesis of rare earth oxide activated Y $(OH)_3$ and Y_2O_3 nanotubes," *Nanotechnology*, vol. 20, pp. 305302–305309, 2009.

[3] J. K. Won, J. K. Sung, K.-S. Lee, M. Samoc, A. N. Cartwright, and P. N. Prasad, "Robust microstructures using UV photopatternable semiconductor nanocrystals," *Nano Letters*, vol. 8, no. 10, pp. 3262–3265, 2008.

[4] H. Liu, L. Wang, S. Chen, and B. Zou, "Effect of concentration on the luminescence of Eu^{3+} ions in nanocrystalline La_2O_3," *Journal of Luminescence*, vol. 126, no. 2, pp. 459–463, 2007.

[5] D. Hreniak, A. Speghini, M. Bettinelli, and W. Strek, "Spectroscopic investigations of nanostructured $LiNbO_3$ doped with Eu^{3+}," *Journal of Luminescence*, vol. 119-120, pp. 219–223, 2006.

[6] E. M. Goldys, K. Drozdowicz-Tomsia, S. Jinjun et al., "Optical characterization of Eu-doped and undoped Gd_2O_3 nanoparticles synthesized by the hydrogen flame pyrolysis method," *Journal of the American Chemical Society*, vol. 128, no. 45, pp. 14498–14505, 2006.

[7] H. Guo, N. Dong, M. Yin, W. Zhang, L. Lou, and S. Xia, "Visible upconversion in rare earth ion-doped Gd_2O_3 nanocrystals," *Journal of Physical Chemistry B*, vol. 108, no. 50, pp. 19205–19209, 2004.

[8] X. Chen, E. Ma, G. Liu, and M. Yin, "Excited-state dynamics of Er^{3+} in Gd_2O_3 nanocrystals," *Journal of Physical Chemistry C*, vol. 111, no. 27, pp. 9638–9643, 2007.

[9] A. Brenier, "Laser-heated pedestal growth of Er^{3+}-doped Gd_2O_3 single crystal fibres and up-conversion processes," *Chemical Physics Letters*, vol. 290, no. 4–6, pp. 329–334, 1998.

[10] L. Laversenne, Y. Guyot, C. Goutaudier, M. T. Cohen-Adad, and G. Boulon, "Optimization of spectroscopic properties of Yb^{3+}-doped refractory sesquioxides: cubic Y_2O_3,Lu_2O_3 and monoclinic Gd_2O_3," *Optical Materials*, vol. 16, no. 4, pp. 475–483, 2001.

[11] F. Vetrone, J. C. Boyer, J. A. Capobianco, A. Speghini, and M. Bettinelli, "Effect of Yb^{3+} codoping on the upconversion emission in nanocrystalline Y_2O_3:Er^{3+}," *Journal of Physical Chemistry B*, vol. 107, no. 5, pp. 1107–1112, 2003.

[12] A. R. West, *Solid State Chemistry and It's Application*, John Wiley & Sons, New York, NY, USA, 1989.

[13] J. D. Corbett, *Solid State Chemistry—Techniques*, Oxford Press, 1992, Edited by A. K. Cheetham and P. Day.

[14] C.-H. Lu, C.-H. Huang, and B.-M. Cheng, "Synthesis and luminescence properties of microemulsion-derived $Y_3Al_5O_{12}$:Eu^{3+} Phosphors," *Journal of Alloys and Compounds*, vol. 473, no. 1-2, pp. 376–381, 2009.

[15] A. Guinier, *X-Ray Diffraction*, Freeman, San Francisco, Calif, USA, 1963.

[16] D. Grier and G. Mc Garthy, Fargo, ND, USA, ICCD, grantin Aid, 1991.

[17] P. H. Klug and L. E. Alexender, *X-Ray Diffraction*, Addision-Wilson, 1974.

[18] N. Zhang, R. Yi, L. Zhou et al., "Lanthanide hydroxide nanorods and their thermal decomposition to lanthanide oxide nanorods," *Materials Chemistry and Physics*, vol. 114, no. 1, pp. 160–167, 2009.

[19] C. Furetta, *Handbook of Thermoluminescence*, World Scientific, Singapore, 2003.

[20] R. Chen and S. W. S. McKeever, *Theory of Thermoluminescence and Related Phenomenon*, World Scientific, Singapore, 1997.

[21] R. Chen and Y. Kirish, *Analysis of Thermally Stimulated Processes*, Pergamon, New York, NY, USA, 1981.

[22] R. K. Tamrakar, "Thermoluminescence studies of copper-doped cadmium sulphide nanoparticles with trap depth parameters," *Research on Chemical Intermediates*, vol. 39, no. 9, pp. 4239–4245, 2013.

[23] R. K. Tamrakar, "UV-irradiated thermoluminescence studies of bulk CdS with trap parameter," *Research on Chemical Intermediates*, 2013.

[24] E. Nakazawa and S. Shionoya, "Cooperative luminescence in $YbPO_4$," *Physical Review Letters*, vol. 25, no. 25, pp. 1710–1712, 1970.

[25] L. Laversenne, Y. Guyot, C. Goutaudier, M. T. Cohen-Adad, and G. Boulon, "Optimization of spectroscopic properties of Yb^{3+}-doped refractory sesquioxides: cubic Y_2O_3,Lu_2O_3 and monoclinic Gd_2O_3," *Optical Materials*, vol. 16, no. 4, pp. 475–483, 2001.

[26] L. Van Pieterson, M. Heeroma, E. De Heer, and A. Meijerink, "Charge transfer luminescence of Yb^{3+}," *Journal of Luminescence*, vol. 91, no. 3, pp. 177–193, 2000.